Ground-state properties of few-Boson system in a one-dimensional hard wall potential with split

Xiangguo Yin,[1] Yajiang Hao,[2] Shu Chen,[2] and Yunbo Zhang[1], *

[1]*Department of Physics and Institute of Theoretical Physics,*
Shanxi University, Taiyuan 030006, P. R. China
[2]*Institute of Physics, Chinese Academy of Sciences, Beijing 100080, P. R. China*
(Date textdate)

We carry out a detailed examination of the ground state property of few-boson system in a one-dimensional hard wall potential with a $\delta-$split in the center. In the Tonks-Girardeau limit with infinite repulsion between particles, we use the Bose-Fermi mapping to construct the exact $N-$particle ground state wavefunction which allows us to study the correlation properties accurately. For the general case with finite inter-particle interaction, the exact diagonalization method is exploited to study the ground-state density distribution, occupation number distribution, and momentum distribution for variable interaction strengths and barrier heights. The secondary peaks in the momentum distribution reveal the interference between particles on the two sides of the split, which is more prominent for large barrier strength and small interaction strength.

I. INTRODUCTION

With the development of laser cooling and optical trapping technology, quasi one-dimensional (1D) cold atom systems have been realized by tightly confining the particle motion in two directions to zero point oscillation [1, 2, 3, 4, 5, 6]. Furthermore, optical dipole forces generated by several crossed, interfering laser beams make it possible to create periodic potentials, and experimentalists are able to trap and control small numbers of particles in optical lattice or double well potential. Meanwhile with the Feshbach resonance technique, the inter-particle scattering length can be easily changed by tuning a magnetic field, which allows the atoms to enter the full regime of interaction from weakly to strongly interacting limit. In particular, a quasi-1D quantum gas of strongly interacting bosons has been observed in the so-called Tonks-Girardeau (TG) regime [3, 4]. These experiment progresses inspire great interest in exploring the properties of bosonic gases in the full interaction regime.

As is well known, the Gross-Pitaviskii (GP) theory is widely adopted in dealing with the system of Bose-Einstein condensations with weak interaction. In spite of its great success in explaining the basic experimental observations, the GP equation is fundamentally based on a mean-field approximation and fails in the strongly correlated systems [7, 8]. For arbitrary interaction from weakly to strongly interacting limit, there exist several theoretical treatments including analytic method, e.g. Bethe ansatz [9, 10, 11, 12, 13], and numerical simulation e.g. the exact diagonalization [14, 15], the multi-configuration time-dependent Hartree (MCTDH) method [16, 17], discrete variable representation (DVR) [18], and so on. Bethe ansatz provides the exact so-lution to some many-body systems including Bose gas [9, 10], Fermi gas [11, 12], Bose-Fermi mixture [13] as well as multi-component cases. In the past several years, though it has made great development in cooperation with other theories and some numerical methods, this analytical method mainly solves the uniform system. On the other hand, numerical techniques provide more information about the many-body system, for example, MCTDH method can not only reveal the ground state property, but also tackle its dynamics [19]. For finite particle interactions no analytical solution to the two-particle problem is known for a finite split barrier in the center. DVR has been used to achieve the discretization of the spatial coordinates for two particles, however, the generalization to more particles are not straightforward [18].

While most theoretical works assume large particle numbers, strongly correlated atomic systems realized in current experiments are limited to systems with a small number of particles [3, 4]. The exact diagonalization method becomes more and more versatile and powerful in dealing with the ground state problem of such "few-body" system. In this paper, we study the ground state properties of a few spinless bosons which are confined in a 1D hard-wall trap and interact via repulsive contact potential. In addition we add a δ-split in the center of the trap potential which may be viewed as a generic model for double well structure or, alternatively, as a good approximation to the problem of a trap with an impurity at the center. While the the optical box trap has been experimentally achieved [20], the δ-split potential may be realized by adding an additional laser in the center of the box trap. By changing the strength of the laser, one can tune the height of the split barrier effectively. In order to get some exact results in the strongly coupling limit, we first investigate the system by Fermi-Bose mapping [21, 22] in the infinite repulsive limit in which the interactions between bosonic particles dominate the physics

*Electronic address: ybzhang@sxu.edu.cn

of the system. Then we use the exact diagonalization method to deal with the situation in the full interaction regime. In particular, the reduced single particle density, momentum distribution and occupation of the natural orbits are illustrated by varying the parameters such as the number of particles, the strength of interaction between particles and the height of split barrier.

This paper is organized as follows. In Sec.II we describe the Hamiltonian of the few-boson system and review the single particle eigenstates. In Sec.III, the TG gas is studied and we will see how the properties of the ground state in this extreme limit reveal the implication of this few-boson system. Subsequently Sec.IV is devoted to the exact diaganolization method to deal with the variable interaction case. Finally we summarize our result in Sec.V.

II. MODEL HAMILTONIAN AND SINGLE-PARTICLE EIGENSTATES

We consider N bosonic atoms of mass m confined in a highly elongated hard wall trap which can be treated as quasi-one dimensional. For the case study of localization of particles, we split the trap by inserting a tunable zero-ranged barrier at the trap center [18]. The atoms interact via a delta potential and the Hamiltonian for this system is ($\hbar = m = 1$)

$$H = \sum_{i=1}^{N} h_i + \sum_{i,j=1(i \neq j)}^{N} g\delta(x_i - x_j), \qquad (1)$$

where the single-particle Hamiltonian h_i is given by

$$h_i = -\frac{1}{2}\frac{\partial^2}{\partial x_i^2} + V(x_i) + \kappa\delta(x_i). \qquad (2)$$

Here $V(x)$ describes a hard wall trap which is zero in the region $(-a, +a)$ and infinite outside. The last term in the single-particle Hamiltonian represents a δ-type barrier located at the origin and we denote the strength of this barrier by a positive parameter κ. Another essential parameter to characterize the system is the one-dimensional interaction strength g which is determined by the modified s-wave scattering length due to the strong transverse confinement [5]. The single-particle Hamiltonian can be exactly solved and the solution can be found in standard textbook and we review the result here again for later computation.

The eigen equation of single-particle Hamiltonian is

$$\left[-\frac{1}{2}\frac{\partial^2}{\partial x^2} + V(x) + \kappa\delta(x) \right] \phi(x) = E\phi(x). \qquad (3)$$

The eigenfunctions are either symmetric or antisymmetric. The analytic symmetric eigenfunctions are

$$\phi_n(x) = \begin{cases} C[\cos(px) - \frac{\kappa}{p}\sin(px)], -a \leq x \leq 0 \\ C[\cos(px) + \frac{\kappa}{p}\sin(px)], 0 \leq x \leq a \end{cases} \qquad (4)$$

Here, C is the normalization constant and p is the wave vector of particle determined by $p/\kappa + \tan(pa) = 0$. The corresponding energy is $E = p^2/2$. By contrast, the antisymmetric eigenfunctions are unaffected by the barrier and vanish at the origin. They are the same as the odd eigenstate of the hard wall trap without split ($\kappa = 0$)

$$\phi_n(x) = \frac{1}{\sqrt{a}}\sin\left[\frac{(n+1)\pi x}{2a}\right], \ n = 1, 3, 5 \cdots \qquad (5)$$

The corresponding energies is determined by $E_n = ((n+1)\pi/2a)^2/2$. In the limit $\kappa \to 0$, energies for symmetric states in unit of $\pi^2/2a^2$ are $E_n = (1/2)^2, (3/2)^2, (5/2)^2, \cdots$, and those for the antisymmetric eigenstates are $E_n = 1, 2^2, 3^2, \cdots$. In the opposite limit, i.e. $\kappa \to \infty$, the former energy series converge towards $E_n = 1, 2^2, 3^2, \cdots$, and each symmetric eigenstate becomes degenerate with the next highest-lying antisymmetric state.

III. TONKS-GIRARDEAU GAS

The infinite interaction between the atoms can be represented as a constraint on the allowed bosonic wavefunction $\Psi(x_1, \cdots, x_N)$.

$$\Psi(x_1, \cdots, x_N) = 0 \quad \text{if } x_i = x_j, 1 \leq i < j \leq N, \qquad (6)$$

which suggests that TG gas may be viewed as a group of "free" bosons governed by the Hamiltonian $\sum_{i=1}^{N} h_i$, while its wavefunction is subjected to the constraint in Eq. (6). One can see immediately that this constraint is equivalent to the exclusive principle for a Fermi system with antisymmetric wavefunctions. Based on this observation Girardeau [21] found the Bose-Fermi mapping theorem that allows one to construct wavefunction for a TG gas from the wavefunction of a free Fermi system. In particular, the wavefunction of the bosonic system $\Psi_B(x_1, \cdots, x_N)$ is related to the non-interacting fermionic wavefunction $\Psi_F(x_1, \cdots, x_N)$ by the mapping

$$\Psi_B(x_1, \cdots, x_N) = A(x_1, \cdots, x_N)\Psi_F(x_1, \cdots, x_N). \qquad (7)$$

The fermionic wavefunction can be constructed from Slater determinant $\Psi_F(x_1, \cdots, x_N) = \sqrt{1/N!}\det_{n=0,j=1}^{N-1,N}(\phi_n(x_j))$ where $\phi_n(x_j)$ are the single particle wavefunctions obtained above. The antisymmetric function $A(x_1, \cdots, x_N)$ is defined as $A(x_1, \cdots, x_N) = \prod_{i>j} sgn(x_i - x_j)$ with sgn the sign function. The TG gas is exactly solvable in this way and one easily see that the single-particle density or the thermodynamic properties are identical for these two systems.

However, quantum correlations considerably differ from each other as can be manifested in the reduced single-particle density (RSPD) or the momentum distribution. Although the exact many-body wave function
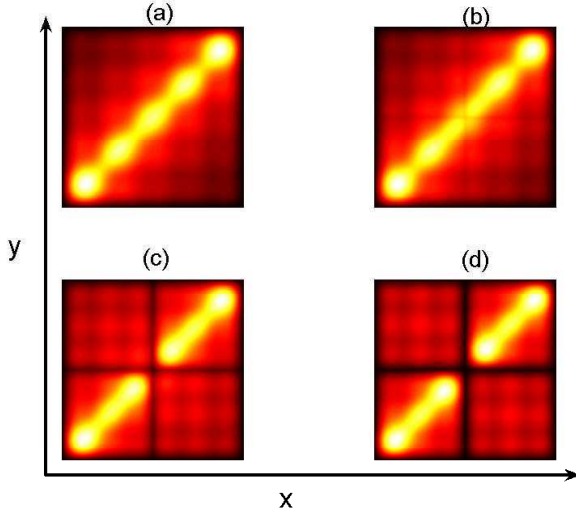
FIG. 1: (Color online) Reduced single-particle density matrix of 5 bosons in TG limt, for barrier strength (a)$\kappa = 0.2$, (b)$\kappa = 2$, (c)$\kappa = 20$, (d)$\kappa = 200$. Each plot spans the range $-a < x, y < a$.

FIG. 2: (Color online) Reduced single-particle density matrix of 6 bosons in TG limt, for barrier strength (a)$\kappa = 0.2$, (b)$\kappa = 2$, (c)$\kappa = 20$, (d)$\kappa = 200$. Each plot spans the range $-a < x, y < a$.

describing TG gas can be written in compact form, it is a difficult task to calculate the RSPD defined as

$$\rho(x, y) = N \int dx_2 \cdots dx_N$$
$$\times \Psi_B^*(x, x_2, \cdots, x_N) \Psi_B(y, x_2, \cdots, x_N) \qquad (8)$$

and the momentum distribution

$$n(k) = \frac{1}{2\pi N} \int_{-\infty}^{+\infty} dx \int_{-\infty}^{+\infty} dy \rho(x, y) \exp(-ik(x - y)) \qquad (9)$$

which is normalized to one. To resolve the difficulty of multi-integration, Pezer and Buljan [24] rewrote the RSPD in terms of the single particle basis

$$\rho(x, y) = \sum_{i,j=1}^{N} \phi_i^*(x) B_{ij}(x, y) \phi_j(y). \qquad (10)$$

The coefficients $B_{ij}(x, y)$ constitute an $N \times N$ matrix $\mathbf{B}(x, y) = (\mathbf{P}^{-1})^T \det \mathbf{P}$ and the entries of the matrix $\mathbf{P}$ are $P_{ij}(x, y) = \delta_{ij} - 2 \int_x^y dx' \phi_i^*(x') \phi_j(x')$, assuming $x < y$ without loss of generality. This scheme enables efficient and exact numerical calculation of quantum correlations in few body systems.

We illustrate the RSPD of 5 particles in Fig. 1 and that of 6 particles in Fig. 2 for four different barrier strengths $\kappa = 0.2, 2, 20, 200$, respectively. The diagonal term $\rho(x, x)$ is nothing but the single-particle density and is normalized to N. For a negligibly small split barrier, Fig.1 (a) and Fig.2 (a) show that the diagonal line have N peaks meaning N density maxima, since the infinite interaction between particles repel each other to occupy different positions. Meanwhile the off-diagonal elements are non-zero, which reflect the correlation between particles. Physically this self correlation $\rho(x, y)$
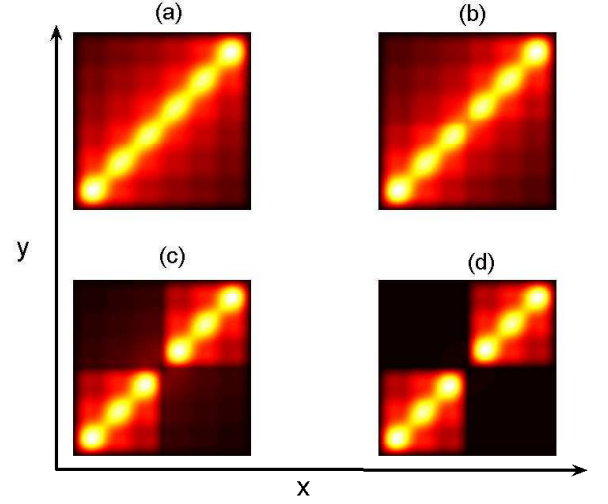
can be viewed as the probability that two successive measurements will find the particles at position x and y, respectively. Increasing the barrier strength, as seen in Fig.1 (b-d) and Fig.2 (b-d), leads to the emergence of a quadrant separation which coincides with the result of Ref. [18]. We note also in this system there appears an interesting parity effect for odd and even number of particles. When N is odd, the middle peak begins to split into two with increasing barrier strength, so the number of density peaks in each well increases from $(N - 1)/2$ to $(N + 1)/2$. When N is even, on the other hand, there are always $N/2$ peaks in each well for any value of barrier height. For a very strong split in the center, e.g. $\kappa = 200$, the off-diagonal quadrants diminish for N is even, while remain nonzero for N is odd. This implies that for odd number of particles, the correlation between the two sides of the split persists for a rather high barrier.

We can explain our result in a way similar to the energy band theory. The barrier in our system splits the hard wall trap into a double-well structure. Just as the extension of two-site Hubbard model to a lattice gives naturally the energy band, one can imagine that the hard wall trap with periodically distributed $\delta-$splits, i.e., Kronig-Penny potential, admits also similar band structure [23]. Each band in our system, however, consists of only two energy levels. The infinite interaction between particles forbids particles to occupy the same level and only two particles are allowed to populate in each energy band. For the ground state, particles occupy the energy levels from the bottom one by one. When N is even, all occupied energy bands are full and the system is in an insulator state, while for N is odd, the highest occupied band is half filled which reminds us the conduction band in metal conductor. Particles occupying that band can move more freely which is the reason for different
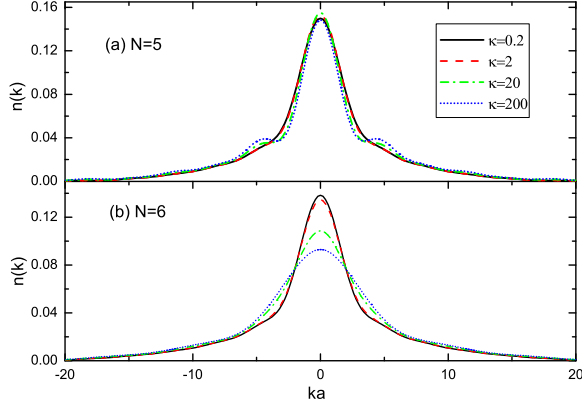
FIG. 3: (Color online) Momentum distribution, $n(k)$, of 5 particles (a) and 6 particles (b) in TG limit for $\kappa = 0.2, 2, 20, 200$. When the number of particles is odd, the secondary peaks appear for increased barrier strength due to the interference of particle in two almost separate wells, while for even, the momentum distribution broaden for increased barrier strength owing to the localization of particles in separate halves of the trap.
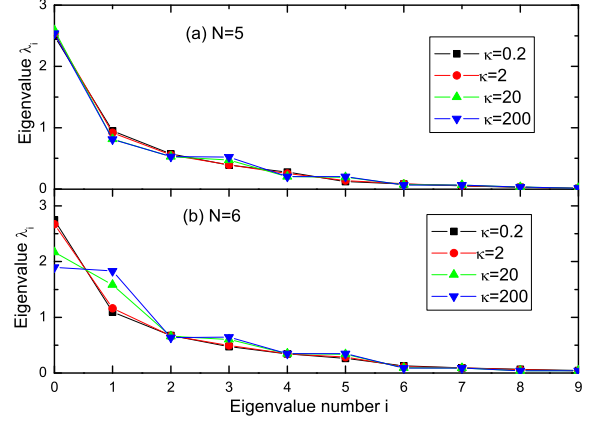

FIG. 4: (Color online) Occupation of the natural orbits λ_i of 5 particles (a) and 6 particles (b) in TG limit for $\kappa = 0.2, 2, 20, 200$. When the number of particles is odd, with the increased barrier strength, the two largest occupations do not change almost while the other nearby two occupations have the same value which form pairs. When N is even, with the increased barrier strength, all nearby two occupations have the same value which also form pairs.

off-diagonal elements of RSPD induced by the parity of particle number.

These results can also be understood in a simpler way. When N is even, each well can keep $N/2$ particles, and the chemical potential can keep balance in two sides of middle barrier. When N is odd, supposed each well is firstly filled with $(N-1)/2$ particles, one would face a dilemma on how to put the last one. The probability of finding the last particle is the same in each well, which keeps the connection between the two wells and leads to non-zero RSPD in off-diagonal quadrant.

To characterize some BEC-like coherence effects in few body system, one usually examine the eigenvalues and eigenfunctions of the RSPD [22]. The eigenfunctions of the RSPD, called the natural orbits $\varphi(x)$ in TG systems

$$\int dy \rho(x, y) \varphi_i(y) = \lambda_i \varphi_i(x), i = 0, 1, 2 \cdots \quad (11)$$

represent a set of effective single-particle states, while eigenvalues λ_i represent their occupation and $\sum_i \lambda_i = N$. The momentum distribution is related to these natural orbits via the relation $n(k) = \sum_i \lambda_i |\mu_i(k)|^2$, where $\mu_i(k)$ denotes the Fourier transformation of $\varphi_i(x)$

$$\mu_i(k) = \int dx \varphi_i(y) \exp(-ikx) / \sqrt{2\pi N}.$$

Fig.3 shows the momentum distribution in the TG limit for four different values of the barrier strength $\kappa = 0.2, 2, 20, 200$. When N is odd, as the barrier strength is increased, the main peak firstly increases, reaches the critical value for a barrier strength, and then begins to decrease thereafter. The secondary peaks appear with increasing strength of barrier. The barrier separates the particles into two half wells, which, however, are not independent but interfere with each other. It is this interference that leads to the appearance of the secondary peaks. When the number of particles increase, the secondary peaks become more and more slight as a result of infinite interaction between particles. When N is even, the momentum distribution becomes broader and broader with increasing barrier strength and the height of peak decreases monotonically, which coincides with earlier observation that $N/2$ particles become localized in each separate half-well and keep balance in the two sides of barrier.

We also present the occupation of the natural orbits for odd and even particles in Fig.4. Clearly the presence of the split in the center will not affect the occupation obviously for odd number of particles. The first and second occupancies remain the same for increasing barrier height, but the third and fourth occupancies tend to form the staircase structure, implying the formation of pairs. Subsequently, the next two occupancies also form pairs, and so on. Contrary to this, for even number of particles, all occupations tend to form pairs with increasing barrier strength due to the degeneracy of energy levels, which is also observed in fermionic TG gas [25]. In the case of odd number of particles, the presence of the last particle prevents the formation of pairs in the the first and second occupations.
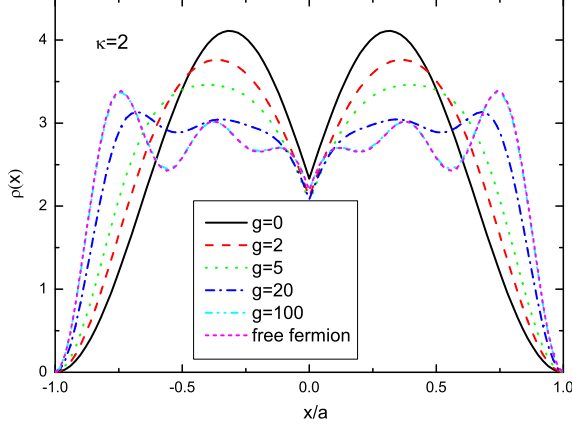
FIG. 5: (Color online) Particle density of five bosons for barrier strength $\kappa = 2$ and different interaction strength $g = 0, 2, 5, 20, 100$. The density becomes flatter and broader with increasing g. In the strong interaction regime new peaks appear gradually and finally the density tends to be the same as that of 5 free Fermions.

IV. VARIABLE INTERACTION STRENGTH

For finite particle interaction, we use exact diagonalization method [14] to deal with the many body Hamiltonian (1), which takes the second quantized form

$$H = \sum_i E_i a_i^\dagger a_i + \frac{1}{2} g \sum_{ijkl} I_{ijkl} a_i^\dagger a_j^\dagger a_k a_l \qquad (12)$$

where $a_i^\dagger (a_i)$ is the bosonic creation (annihilation) operator for a particle in the single particle energy eigenstate $\phi_i(x)$. The interaction integration parameters I_{ijkl} are calculated through $I_{ijkl} = \int dx \phi_i(x) \phi_j(x) \phi_k(x) \phi_l(x)$. The Hamiltonian is diagonalized in the subspace of the energetically lowest eigenstates of non-interaction many-particle system. Some exact results for a pair of bosons have been obtained in ref. [18] and our calcualtion for even number of particles implies similar behaviours in the relevant physical quantities. We will concentrate on the results for odd number of bosons $N = 5$ considering 26 single particle eigenstates in the following.

Let's first discuss the particle density, $\rho(x) = \left\langle \hat{\Psi}^\dagger(x) \hat{\Psi}(x) \right\rangle = \sum_{i,j} \left\langle a_i^\dagger a_j \right\rangle \phi_i(x) \phi_j(x)$ where the mean value is calculated on the ground state of Hamiltonian (12). Without loss of generality, we choose the barrier strength $\kappa = 2$. Fig.5 shows the particle density for variable interaction strength $g = 0, 2, 5, 20, 100$. Because of the presence of the central barrier, the density in the middle position appears to be lower than its nearby region. For noninteracting bosons, there is one peak on either side of the barrier respectively. As the interaction strength is increased, the particle density begins to
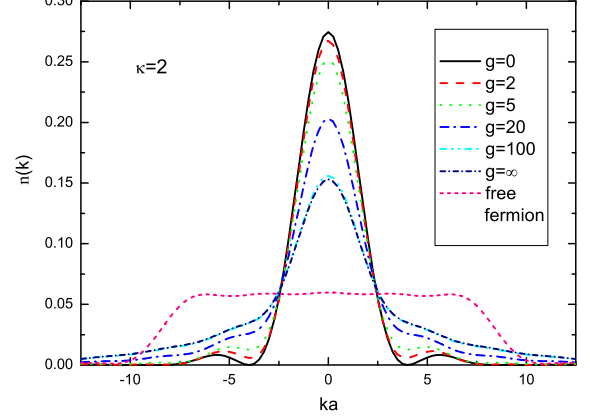

FIG. 6: (Color online) Momentum distribution of five bosons for different interaction strength g. The secondary peaks disappear with increasing interaction strength which hinders the interference of the particles in two separate half-wells.

spread out and becomes flatter, while the height of two peaks is decreased. New small peaks appear for certain interaction and finally the density tends to be the same as that for free fermion system.

The momentum distribution for finite interaction is now calculated as $n(k) = \left\langle \hat{\Pi}^\dagger(k) \hat{\Pi}(k) \right\rangle / N$ and is normalized to one. Here $\hat{\Pi}(k)$ annihilates a boson with momentum k and can be expanded upon the Fourier transformation of single particle eigenstates $\phi_i(x)$. Fig.6 shows the momentum distribution for the same values of interaction strength as in Fig.5. We find, as the interaction is increased, the secondary peaks disappear gradually and the central peak becomes lower and broader. This result proves that the interaction will diminish the interference between two wells. The momentum distribution is identical for $g = 100$ and TG limit $g = \infty$ which is calculated by the Fermi-Bose mapping in the above section. In the TG case, the long tail appears because the higher energy levels may been occupied by some particles owing to the infinity repel interaction, which agrees with general nature of a TG gas. This is in strike contrast with the main feature of momentum distribution for 5 free fermions which takes the plateau shape composed of 5 peaks and without the long tail.

We also present the result for occupation number distribution $\langle n_i \rangle = \left\langle a_i^+ a_i \right\rangle$ which is different from the occupation of natural orbits mentioned above. The occupied states here are single particle wavefunctions in the trap, while natural orbits are eigenfunctions of the RSPDM. As can be seen in Fig.7, with increasing g, the bosons occupy not only the ground state but also some low-lying excited states. The occupation number in the lower state are always larger than that in the next higher one, which is different with particles in the harmonic trap [14]. In
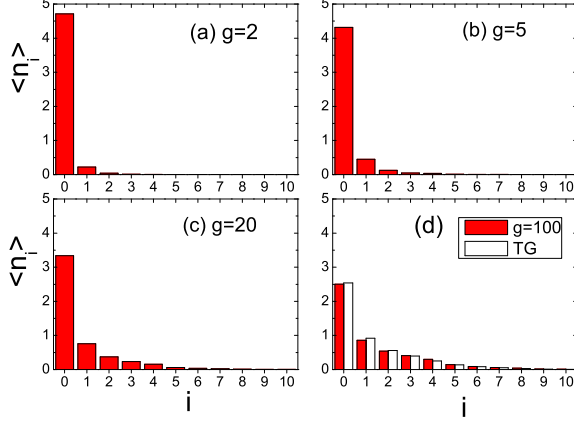
FIG. 7: (Color online) Occupation number distribution of five bosons for different interaction strength g. On each state in (d), the left solid part represents $g = 100$ and the right hollow part shows the TG case. With increasing g the bosons leave the ground state and occupy excited states. The occupation number in the lower state are always larger than that in the next higher state.

FIG. 9: (Color online) Momentum distribution of five bosons for varying inter-particles interaction strength $g = 0$ (a), 2 (b), 20 (c), ∞ (d). Within each plot the distribution is considered for 4 different values of the barrier strength: $\kappa = 0.2, 2, 20, 200$. Secondary peaks appear with increasing barrier strength, while disappear for increasing interaction strength.
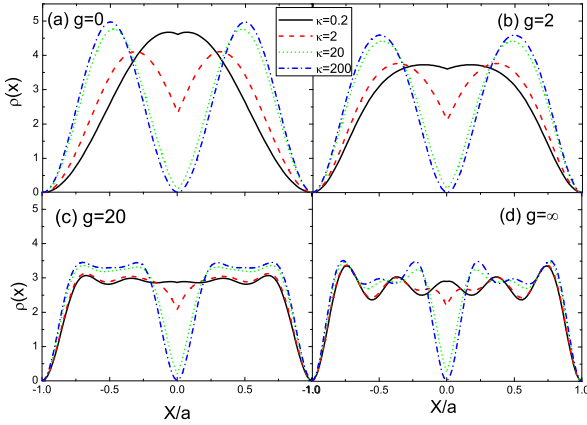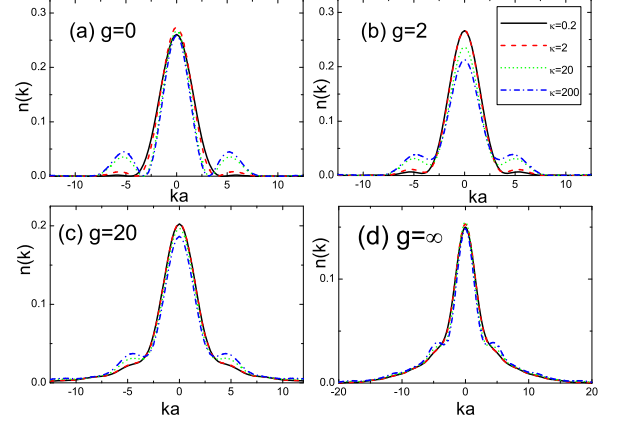

FIG. 8: (Color online) Particle density distribution of five bosons for varying inter-particles interaction strength $g = 0$ (a), 2 (b), 20 (c), ∞ (d). Particles are separated into two parts with increasing barrier strength.

The last knob to control the system is the variable barrier strength of the split. Fig.8 shows the particle density distribution for four inter-particle interaction strengths $g = 0, 2, 20, \infty$ and four values of barrier strengths $\kappa = 0.2, 2, 20, 200$. As the barrier strength is increased, the density in middle area is decreasing while the density in other area is increasing for any interaction. The barrier therefore divides the particles into two areas regardless of the interaction. It is more constructive to say more words on the secondary peaks in the momentum distribution, which has already been shown in Fig.6. Physically, the interference between particles split into the two separate half-wells gives rise to these peaks, which reminds us the famous double-slit arrangement. Fig.9 (a) shows the momentum distribution of 5 non-interacting particles ($g = 0$) for varying κ. In this case the momentum distribution is given by the square of the single-particle wave-function in momentum space. So we can write it out analytically

$$
\begin{aligned}
n(p) &= C(\frac{\sin{(k+p)}}{k+p} + \frac{\sin{(k-p)}}{k-p} + \frac{\kappa}{k}\frac{1-\cos{(k+p)}}{k+p} \\
&+ \frac{\kappa}{k}\frac{1-\cos{(k-p)}}{k-p})^2
\end{aligned}
\tag{13}
$$

with C is a normalization factor. The secondary peaks can be seen more and more clearly with increasing strength of barrier. Strength of the barrier causes the spreading of the particle-density in two wells, which in turn leads to a narrowing of momentum peaks. For finite interaction strength, Fig.9 (b-d) show similar tendency for the central and secondary peaks. The disappearance of the secondary peaks with increasing interaction

the harmonic trap, single-particle states with even parity are stronger occupied compared to those with odd parity. The difference between our double well and single well structure comes from the fact that odd parity states can never feel the existence of the split in the center. In Fig.7 (d) we compare these two kinds of occupations of single particle states and natural orbits and find that they almost have the same value in the corresponding state though the details are not completely identical.

strength can be attributed to the increased localization of the particles, analogous to the superfluid-insulator transition of the Bose-Hubbard model in optical lattice studies [26].

V. CONCLUSION

In conclusion, we have studied the ground state property of few bosons in a hard wall trap with $\delta-$type split in the center. Based on the Fermi-Bose mapping, the reduced single-particle density and the momentum distribution of odd ($N = 5$) and even ($N = 6$) bosons are illustrated and explained in TG limit. The off-diagonal quadrants representing the interference between two half wells remain nonzero for N is odd, while disappear for N is even. For finite interaction strength, the exact diago-

nalization method enables us to manipulate the system in several ways, including variable number of particles, interaction strength, barrier height of the split, etc. The interference between particles on the two sides of the split manifests itself in the secondary peaks of the momentum distribution, emerging with increasing barrier strength κ, while vanishing for increasing interaction strength g.

[1] A. Görlitz, et.al., Phys. Rev. Lett. **87**, 130402 (2001).
[2] H. Moritz, T. Stöferle, M. Köhl, and T. Esslinger, Phys. Rev. Lett. **91**, 250402 (2003); T. Stöferle, H. Moritz, C. Schori, M. Köhl, and T. Esslinger, ibid. **92**, 130403 (2004).
[3] B. Paredes, A. Widera, V. Murg, O. Mandel, S. Fölling, I. Cirac, G. V. Shlyapnikov, T. W. Hänsch, and I. Bloch, Nature **429**, 277 (2004).
[4] T. Kinoshita, T. Wenger, and D. S. Weiss, Science **305**, 1125 (2004).
[5] M. Olshanii, Phys. Rev. Lett. **81**, 938 (1998).
[6] B. L. Tolra, K. M. O'Hara, J. H. Huckans, W. D. Phillips, S. L. Rolston, and J. V. Porto, Phys. Rev. Lett. **92**, 190401 (2004).
[7] E. B. Kolomeisky, T. J. Newman, J. P. Straley, and X. Qi, Phys. Rev. Lett. **85**, 1146 (2000).
[8] S. Chen and R. Egger, Phys. Rev. A. **68**, 063605 (2003).
[9] E. H. Lieb and W. Liniger, Phys. Rev. **130**, 1605 (1963).
[10] Y. Hao, Y. Zhang, J.-Q. Liang, and S. Chen, Phys. Rev. A **73**, 063617 (2006).
[11] C. N. Yang, Phys. Rev. Lett. **19**, 23 (1967); M. Gaudin, Phys. Lett. **24A**, 55 (1967).
[12] Y. Hao, Y. Zhang, and S. Chen, Phys. Rev. A **76**, 063601 (2007).
[13] C. K. Lai and C. N. Yang, Phys. Rev. A **3**, 393 (1971); A. Imambekov and E. Demler, ibid. **73**, 021602(R) (2006).
[14] F. Deuretzbacher, K. Bongs, K. Sengstock, and D.

Pfannkuche, Phys. Rev. A **75**, 013614 (2007).
[15] Y. Hao and S. Chen, arXiv: 0804.1991 .
[16] O. E. Alon, and L. S. Cederbaum, Phys. Rev. Lett. **95**, 140402 (2005); O. E. Alon, A. I. Streltsov, and L. S. Cederbaum, Phys. Rev. A **77**, 033613 (2008).
[17] S. Zöllner, H.-D. Meyer, and P. Schmelcher, Phys. Rev. A **74**, 053612 (2006); ibid. **75**, 043608 (2007).
[18] D. S. Murphy, J. F. McCann, J. Goold, and T. Busch, Phys. Rev. A **76**, 053616 (2007).
[19] S. Zöllner, H.-D. Meyer, and P. Schmelcher, Phys. Rev. Lett. **100**, 040401 (2008).
[20] T. P. Meyrath, F. Schreck, J. L. Hanssen, C.-S. Chuu, and M. G. Raizen, Phys. Rev. A **71**, 041604(R) (2005).
[21] M. Girardeau, J. Math. Phys. **1**, 516 (1960); M. D. Girardeau and E. M. Wright, Phys. Rev. Lett. **84**, 5691 (2000).
[22] M. D. Girardeau, E. M. Wright, and J. M. Triscari, Phys. Rev. A **63**, 033601 (2001).
[23] Y. Lin and B. Wu, Phys. Rev. A **75**, 023613 (2007).
[24] R. Pezer and H. Buljan Phys. Rev. Lett. **98**, 240403 (2007).
[25] M. D. Girardeau and E. M. Wright, Phys. Rev. Lett. **95**, 010406 (2005).
[26] M. Greiner, O.Mandel, T.Esslinger, T. W. Hänsch, I. Bloch, Nature **415**, 39 (2002).